Inhibition of the cell cycle is required for convergent extension of the paraxial mesoderm during *Xenopus* neurulation

Walter F. Leise, III[1,*] and Paul R. Mueller[2,†]

[1]Department of Biochemistry and Molecular Biology, University of Chicago, 924 East 57th Street, Chicago, IL 60637, USA
[2]Department of Molecular Genetics and Cell Biology, Center for Molecular Oncology, and Committees on Developmental Biology, Cancer Biology, and Genetics, University of Chicago, 924 East 57th Street, Chicago, IL 60637, USA
*Present address: Abbott Laboratories; Abbott Park, IL 60064, USA
†Author for correspondence (e-mail: pmueller@midway.uchicago.edu)

Accepted 22 December 2003

Development 131, 1703-1715
Published by The Company of Biologists 2004
doi:10.1242/dev.01054

Summary

Coordination of morphogenesis and cell proliferation is essential during development. In *Xenopus*, cell divisions are rapid and synchronous early in development but then slow and become spatially restricted during gastrulation and neurulation. One tissue that transiently stops dividing is the paraxial mesoderm, a dynamically mobile tissue that forms the somites and body musculature of the embryo. We have found that cessation of cell proliferation is required for the proper positioning and segmentation of the paraxial mesoderm as well as the complete elongation of the *Xenopus* embryo. Instrumental in this cell cycle arrest is Wee2, a Cdk inhibitory kinase that is expressed in the paraxial mesoderm from mid-gastrula stages onwards. Morpholino-mediated depletion of Wee2 increases the mitotic index of the paraxial mesoderm and this results in the failure of convergent extension and somitogenesis in this tissue. Similar defects are observed if the cell cycle is inappropriately advanced by other mechanisms. Thus, the low mitotic index of the paraxial mesoderm plays an essential function in the integrated cell movements and patterning of this tissue.

Key words: *Xenopus*, Wee1, Wee2, Cdk, Cell cycle, Morphogenesis, Convergent extension, Somitogenesis

Introduction

During embryogenesis, there must be balance between cell proliferation and other developmental events. Although cell division is required to produce a sufficient number of cells for the functional organization of an embryo, the process of cell division is incompatible with other events such as cell type specification, cell differentiation and certain types of cell movements (Vidwans and Su, 2001). In vertebrates, cell movement is particularly important during gastrulation and neurulation. It is during this period of development when the basic body pattern is established. Specifically, the three germ layers, the elongated shape and the segmented pattern of the embryo are laid down for future development.

Convergent extension, or the simultaneous narrowing and lengthening of a tissue, is one of the key developmental mechanisms that shapes many features of embryos (Keller, 2002; Wallingford et al., 2002). Early in *Xenopus* embryogenesis, gastrula-stage convergent extension assists in the involution of the axial and paraxial mesoderm over the dorsal lip (Keller et al., 2000). This movement positions these mesodermal tissues underneath the presumptive neural plate on the dorsal side of the embryo. Later during neurulation, convergent extension causes the axial mesoderm, the paraxial mesoderm and the neural plate to delineate from each other, thicken and elongate. As these tissues elongate, the rest of the embryo elongates with them.

During convergent extension, individual cells within a specified group move between each other in a single orientation (convergence) and this causes the tissue encompassing the group of cells to elongate in an orientation perpendicular to that of the convergence (extension) (Keller, 2002; Keller et al., 2000; Wallingford et al., 2002). The important point is that this is an integrated cell movement that requires the coordinated action of all cells within the group or tissue. The planar cell polarity (PCP) pathway is instrumental in coordinating this process in vertebrates (Keller, 2002; Wallingford et al., 2002). PCP requires the action of specific Wnts acting through the disheveled protein in a β-catenin-independent manner. Numerous studies in *Xenopus* and zebrafish have established that mutation or mis-expression of Wnts, Wnt receptors or downstream effectors disrupts cell polarization, cell elongation and cell adhesion (Myers et al., 2002; Sokol, 1996; Tada and Smith, 2000; Wallingford and Harland, 2001; Wallingford et al., 2000). Without these specific cell morphologies, convergent extension in the axial mesoderm, paraxial mesoderm and neuronal tissue fails resulting in foreshortened and mis-shapen embryos.

Concomitant with the onset of gastrulation and convergent extension, cells of the dorsal mesoderm stop dividing in *Xenopus* (Cooke, 1979; Hardcastle and Papalopulu, 2000; Saka and Smith, 2001). This absence of proliferation continues into neurulation as the dorsal mesoderm delineates into axial and paraxial mesoderm. The cells of the axial mesoderm (notochord) are thought not to divide again, while the cells of

the paraxial mesoderm reenter the cell cycle, but only after a somite has formed (Saka and Smith, 2001). Interestingly, as long as a *Xenopus* embryo has begun gastrulation, artificially blocking the cell cycle at the whole embryo level has little effect on the continuation of gastrulation, neurulation or somitogenesis (Anderson et al., 1997; Cooke, 1973; Harris and Hartenstein, 1991). Although these embryos eventually die, these key morphological events continue unabated in the absence of cell proliferation.

Numerous mechanisms are used to inhibit progression through the cell cycle (Morgan, 1997). Ultimately, these function by regulating the activity of the cyclin dependent kinases (Cdks). These mechanisms include the binding of Cdk inhibitory factors (CKIs) and post-translational phosphorylation. In a developmental context, CKIs have been shown to play important roles in terminal differentiation. For example, the *Xenopus* CKI (p27Xic1) is required for differentiation of muscle and neuronal tissues (Carruthers et al., 2003; Vernon et al., 2003; Vernon and Philpott, 2003). Cell cycle progression can also be blocked through inhibitory phosphorylation of the Cdks. This type of regulation is commonly used to control entry into mitosis and is dependent on the balance of the inhibitory Wee kinase activity and the activating Cdc25 phosphatase activity.

Recently, we identified Wee2, a developmentally regulated member of the Wee family of kinases (Leise and Mueller, 2002), in *Xenopus*. Wee2 is one of three Wee kinase family members that have been found in all vertebrates examined, the others being Wee1 and Myt1. Each of these kinases prevents cell cycle progression by phosphorylating and thus inhibiting the activity of the Cdks. However, these kinases differ from each other in their specific activities, subcellular localization, and temporal and spatial patterns of expression during development (Leise and Mueller, 2002; Morgan, 1997). Wee1 is exclusively expressed as a maternal gene product and its mRNA and protein disappear during gastrulation and neurulation, respectively. Myt1 has both maternal and zygotic expression. In the developing embryo, Myt1 is predominantly expressed in neuronal tissues. Finally, Wee2 is expressed principally in the zygote, reaching high levels of expression by the end of gastrulation. Significantly, the Wee2 transcript is localized to the paraxial mesoderm during gastrulation and neurulation, making Wee2 a possible candidate for causing the low mitotic index in the paraxial mesoderm.

In this study, we have found that Wee2-mediated inhibition of the cell cycle is required for the proper positioning and segmentation of the paraxial mesoderm as well as the complete elongation of the *Xenopus* embryo. Depletion of Wee2 causes an increase in the mitotic index of paraxial mesoderm and prevents convergent extension of this tissue during neurulation. Despite these defects, the early differentiation of the paraxial mesoderm into muscle remains normal. Importantly, the convergent extension defect can be rescued by replacing the depleted, endogenous Wee2 with microinjected Wee2 mRNA. Finally, other mechanisms that upset the balance of inhibitory Cdk phosphorylation and advance the cell cycle cause the same defects as Wee2 depletion. Together, our results suggest that active cell proliferation is incompatible with integrated tissue movements that are used during morphogenesis.

Materials and methods

Morpholino design and testing, plasmid construction, and mRNA translation

Two morpholino antisense oligonucleotides, W2MO.1 (GCCAGA-GAGATCATTATCCAGTGAC) and W2MO.2 (AGACTCATA-GTGCGGCGGTGACACG), were designed to the 5′UTR of *Xenopus* Wee2 (Leise and Mueller, 2002) and were obtained (Gene Tools) along with the standard control morpholino, CMO (CCTCTTACCTCAGTTACAATTTATA). To test these morpholinos in vitro, 200 ng of 5′UTR-Wee2-GFP mRNA was mixed with 400 ng of CMO, W2MO.1, W2MO.2, or water, and then translated with a Rabbit Reticulocyte Lysate System (Promega) in the presence of Trans[^{35}S]-Label (ICN Biochemicals) and subsequently processed for autoradiography.

pCS2-5′UTR-Wee2-GFP was made by subcloning the first 865 bp (including the 5'UTR) of Wee2 cDNA into pCS2+eGFP Bgl2 (gift of David Turner) to make an in frame fusion of Wee2 and GFP. pXenGST-Wee2 was made by subcloning the coding region of Wee2 into pXen1 (MacNicol et al., 1997) (gift of Angus MacNicol). The coding regions of human CDK2 (Gu et al., 1992) and CDK2 AF (Thr14 change to Ala, Tyr15 change to Phe) (Costanzo et al., 2000) (gifts from David Morgan and Jean Gautier, respectively) were amplified by PCR and subcloned into pCS2+ (Turner and Weintraub, 1994) to create pCS2-HCdk2 and pCS2-HCdk2AF. The coding regions of wild-type (WT) and phosphatase-dead (PD) versions of *Xenopus* Cdc25A and Cdc25C (Kim et al., 1999) (gifts of James Maller) were amplified by PCR and subcloned into pCS2+eGFP Bgl2 to create eGFP fusions. Subsequently, the eGFP-Cdc25 fusions were subcloned into pCARGFP (Kroll and Amaya, 1996) (gift of Kristen Kroll) replacing the GFP of the vector with that from pCS2+eGFP Bgl2 to create pCARD-eGFP-Cdc25A WT, pCARD-eGFP-Cdc25A PD, pCARD-eGFP-Cdc25C WT and pCARD-eGFP-Cdc25C PD. All amplified constructs were confirmed by sequencing. Cdk2 WT, Cdk2 AF, eGFP, Wee2 and 5′UTR-Wee2-GFP capped mRNAs were prepared from pCS2-HCdk2, pCS2-HCdk2AF, pCS2+eGFP Bgl2, pXenGST-Wee2 and pCS2-5′UTR-Wee2-GFP as described (Sive et al., 2000).

Microinjection of antisense morpholino, mRNA or DNA into *Xenopus* embryos and dorsal explants

Microinjections were performed as described (Leise and Mueller, 2002). In all experiments, non-injected siblings were processed concurrently and exactly as injected embryos. For all morpholino injections, morpholinos were resuspended in injection buffer [0.1×MBS (Sive et al., 2000) modified to contain twice as much HEPES] immediately before use at a morpholino concentration of 2-4 ng/nl. For unilateral morpholino injections, 500 pg of eGFP mRNA was added to the injection mix, to identify the injected side. For the morpholino rescue experiment, the indicated amount of GST-Wee2 mRNA was added to the injection mix. The mRNA and DNA injections were performed as described (Leise and Mueller, 2002). Dorsal explants were dissected from stage 12.5/13 embryos and processed as described (Wilson et al., 1989) except that dissections and incubations were in Danilchik's for Amy (DFA) buffer (Sater et al., 1993) and the endoderm was left attached to the explants.

Antibody production, endogenous protein isolation, immunoprecipitation, and western analysis

Recombinant, full-length Wee2 protein (Leise and Mueller, 2002) was used to immunize rabbits (Covance). The αWee2 antibody was purified by affinity chromatography against the first 222 amino acids of Wee2 as described (Mueller et al., 1995a). Total protein was extracted from *Xenopus* embryos at the indicated stages of development (Nieuwkoop and Faber, 1994) in extraction buffer as described (Hartley et al., 1996). Samples (100 μg) were either processed for western analysis directly, or first subjected to Wee2

immunoprecipitation from stage specific supernatants (1 mg) using αWee2 antibodies and then processed for Western analysis as described (Mueller et al., 1995a) using αWee2, αPSTAIRE (αCdk1/2) (Santa Cruz) or αMyt1 (Mueller et al., 1995b).

Whole mount in situ hybridization, immunocytochemistry, sectioning, nuclei staining, and paraxial mesoderm volume determination

Whole-mount in situ hybridization was performed as described (Leise and Mueller, 2002) using probes specific for MyoD (Dosch et al., 1997) (gift of Christof Niehrs), XNot (von Dassow et al., 1993) (gift of David Kimelman), Sox3 (Zygar et al., 1998) (gift of Sally Moody), muscle actin (MA) (Mohun et al., 1988) and myosin heavy chain (MHC) (Radice and Malacinski, 1989) (gift of Anna Philpott), GFP and Wee2 (Leise and Mueller, 2002). Whole-mount immunocytochemistry against phospho-histone H3 (αPH3) (Upstate Biotechnology) was performed as described (Leise and Mueller, 2002), except that the pre-incubation was performed at 4°C for 1 hour and the color reaction was performed at 4°C overnight. MyoD (20 μM), XNot (20 μM) and αPH3 (10 μM) stained embryos were subjected to paraffin sectioning as described (Leise and Mueller, 2002; Sive et al., 2000). Composite images of αPH3 stained sections were generated as described (Leise and Mueller, 2002). SYTOX Green (Molecular Probes) nuclear staining was performed on mounted MyoD and XNot sections as described (Newman and Krieg, 2002). Nuclei were counted using a Zeiss AxioScope with a 20× objective. The volume of the paraxial mesoderm was calculated in Photoshop by determining the number of pixels contained in the MyoD-positive region of every section of transversely and sagittally cut embryos, and then summing the number of pixels of all sections.

RNA isolation and RT-PCR

Total RNA was extracted from *Xenopus* embryos in groups of 10 embryos using the RNAeasy RNA Mini isolation kit (Qiagen) as per the manufacturer's recommendations. cDNA was prepared using an oligo dT primer as described (Leise and Mueller, 2002). RT-PCR was performed as described (Steinbach and Rupp, 1999) using the cycling conditions described (http://www.hhmi.ucla.edu/derobertis/index.html). The linear range for each primer was empirically determined (25 cycles for MA and ODC, 30 cycles for MyoD, XNot, Vent1 and MHC), and the lack of DNA contamination was confirmed by RT– reactions. Primers used were MHC (Vernon and Philpott, 2003), MA (Stutz and Spohr, 1986), MyoD (Hopwood et al., 1989), ODC (Agius et al., 2000), XNot (Gont et al., 1993) and Vent1 (Gawantka et al., 1995).

Results

Wee2 protein prevents the paraxial mesoderm from entering mitosis

The cells of most tissues in the *Xenopus* embryo are proliferating during gastrulation and neurulation. Notable exceptions are the dorsal mesoderm during gastrulation and the axial and paraxial mesoderm during neurulation. These tissues have a very low mitotic index and may be arrested in G2 (Cooke, 1979; Saka and Smith, 2001). Wee2, a potent inhibitor of the cell cycle, is first expressed in the dorsal and paraxial mesoderm during gastrulation and neurulation, respectively (Leise and Mueller, 2002). This can be observed in sagittal sections of stage 12.5 and 18 embryos (Fig. 1A). At both of these stages there is a strong correlation between the absence of cells undergoing mitosis, as measured by presence of phosphorylated histone H3, and the expression pattern of Wee2 (compare panels 1 and 2, and 3 and 4). This correlation raises the possibility that Wee2 may be responsible for the low mitotic index found in the paraxial mesoderm.

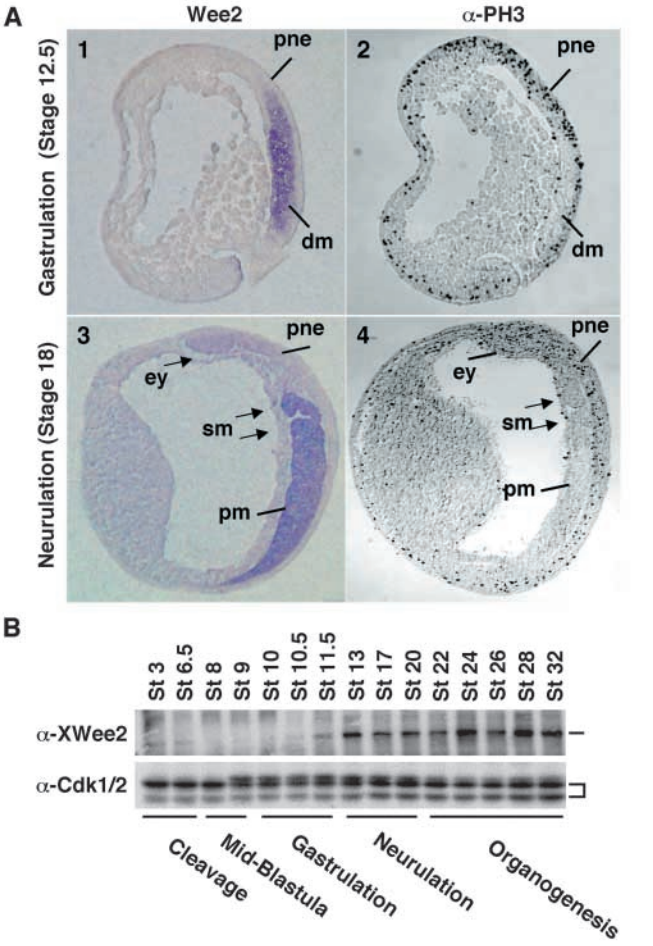

Fig. 1. Wee2 expression correlates with the lack of mitotic cells within the dorsal and paraxial mesoderm. (A) Panels 1 and 3 are sagittal sections of representative stage 12.5 and 18 embryos that were subjected to in situ hybridization for Wee2. Panels 2 and 4 are composite images of 10 serial sagittal sections of representative stage 12.5 and 18 embryos that were subjected to whole-mount immunocytochemistry against phospho-histone H3 (αPH3). Note the absence of mitotic cells (black dots) in the dorsal and paraxial mesoderm. Dorsal towards the right, anterior towards the top. pne, presumptive neural ectoderm; dm, dorsal mesoderm; pm, paraxial mesoderm; ey, eye anlage; sm, somite. (B) Wee2 protein is expressed from mid-gastrula stages onwards. Indicated developmental stages were subject to αWee2 and αCdk1/2 western analysis.

Previous in situ and northern analysis showed that although Wee2 mRNA is nearly undetectable early in development, its levels increase significantly with the onset of gastrulation (Leise and Mueller, 2002). Using an antibody against Wee2, we found that the endogenous Wee2 protein closely parallels the temporal expression of Wee2 mRNA (Fig. 1B). Wee2 protein is readily detectable by mid-gastrulation, increases during neurulation, and then continues to be detectable throughout development. During this period, two substrates of Wee2, Cdk1 and Cdk2 (Leise and Mueller, 2002) (data not shown), remain present at relatively constant levels (Fig. 1B). The combined in situ, northern and western results suggest that the Wee2 protein is spatially restricted to the paraxial

mesoderm from mid-gastrulation to at least late neurulation, and may therefore be amenable to depletion by blocking its translation during development.

To test whether Wee2 might be the direct cause of the low mitotic index found in the paraxial mesoderm, we used morpholino based antisense technology to reduce the level of Wee2 protein. Morpholino oligonucleotides inhibit the translation of specific targets by blocking access of the translational machinery to the 5′UTR of a mRNA target transcript with high specificity and low toxicity (Heasman, 2002). We designed two antisense morpholinos (W2MO.1 and W2MO.2) to the 5′UTR of Wee2. We first tested these in an in vitro translation assay using a Wee2 5′UTR-GFP fusion construct as the transcript. Unlike the control morpholino (CMO), both W2MO.1 and W2MO.2 reduced the translation of this mRNA (Fig. 2A). In this assay, W2MO.1 was more efficient than W2MO.2. We next asked whether the morpholinos could reduce the accumulation of Wee2 protein in vivo. Embryos were either left untreated (sibling) or treated with the various morpholinos at the two-cell stage by microinjection of both blastomeres. These embryos were allowed to develop until the controls had reached either stage 13 or stage 18, and were then processed for western analysis. Both of the Wee2 targeted morpholinos reduced the accumulation of Wee2 protein at stage 13 (data not shown) and at stage 18 (Fig. 2B). As with the in vitro assay, W2MO.1 reduced translation more efficiently than W2MO.2. The reduction of the endogenous level of Wee2 protein was dependent on the dose of Wee2 morpholino (Fig. 2C). At the highest level of the more efficient morpholino, W2MO.1, we observed an almost complete abrogation of Wee2 protein accumulation in late neurulating (stage 18) embryos. At earlier times in development (stage 13), half as much morpholino could be used to obtain the same level of Wee2 protein

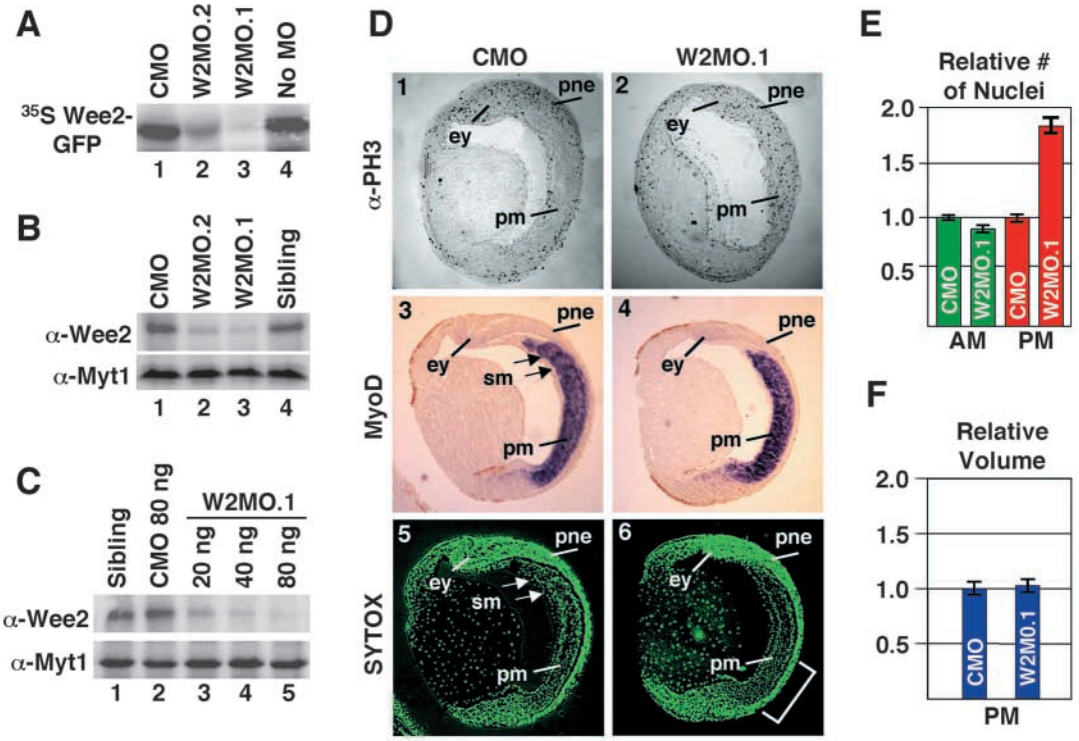

Fig. 2. The low mitotic index of the paraxial mesoderm requires Wee2. (A) Wee2 targeted morpholinos (W2MO.1 and W2MO.2), but not a control morpholino (CMO) or water (No MO), blocked the in vitro translation of a mRNA containing the 5′UTR of Wee2 fused to GFP. (B) W2MO.1 and W2MO.2, but not CMO, reduce the endogenous levels of the Wee2 protein. 40 ng of CMO, W2MO.2 or W2MO.1 were microinjected into each cell of two-cell embryos. Sibling is a non-injected control. At stage 18, these embryos were analyzed for Wee2 and Myt1 protein levels by western analysis. (C) W2MO.1 reduces the level of endogenous Wee2 protein in a dose-dependent manner. 40 ng CMO; or 10, 20 or 40 ng W2MO.1 were microinjected into each cell of two-cell embryos and then processed as in B. The total amount of morpholino injected is indicated. (D) Embryos were microinjected as in B with CMO (odd panels) or W2MO.1 (even panels), and allowed to develop to stage 18. Panels 1 and 2 are composite images of eight serial sagittal sections from representative embryos that were processed for PH3 staining. Note the increase in mitotic cells (black dots) within the paraxial mesoderm of Wee2-depleted embryos (panel 2). Panels 3 and 4 are sagittal sections of embryos processed for MyoD in situ analysis. These same MyoD sections were subsequently stained with SYTOX Green to visualize the nuclei (panels 5 and 6). Nuclei in the paraxial mesoderm appear dimmer owing to the MyoD staining. Note the absence of somites in Wee2-depleted embryos. Labels and orientation as in Fig. 1A. (E) Depletion of Wee2 protein causes cell proliferation within the paraxial mesoderm but not the axial mesoderm. The total number of nuclei within the paraxial and axial mesoderm was determined by counting all nuclei within the MyoD- (paraxial mesoderm, PM) or XNot- (axial mesoderm, AM) positive regions of representative embryos that were microinjected with either CMO or W2MO.1. Every section of both transversely (MyoD and XNot) and sagittally (MyoD) cut embryos was counted and totaled. Data are -fold change from the control (CMO=1). (F) The total volume of MyoD-expressing tissue does not change with depletion of Wee2 protein. The same transverse and sagittal MyoD stained sections used in E were used to determine the area of MyoD expression. Data are -fold change from the control (CMO=1).

reduction (data not shown). Importantly, the Wee2-directed morpholinos reduced the level of endogenous Wee2 protein specifically as they had no effect on a related protein, Myt1 (Fig. 2B,C) or an unrelated protein, p90 Rsk (data not shown). In all cases, the highest dose of control morpholino (CMO) had no effect.

Finally, we asked whether the reduction in Wee2 protein level could change the mitotic index of the paraxial mesoderm. W2MO.1 or CMO were microinjected into both blastomeres of two-cell embryos and these were allowed to develop until controls had reached stage 18. The embryos were processed for immunocytochemistry against phospho-histone H3 to detect mitotic cells (Fig. 2D, panels 1 and 2), and for in situ analyses against MyoD (panels 3 and 4) and XNot (data not shown) to delineate the paraxial and axial mesoderm, respectively (Dosch et al., 1997; Saka and Smith, 2001; von Dassow et al., 1993). Subsequently, the MyoD and XNot sections were treated with the nuclear dye SYTOX Green to detect the position and number of nuclei (panels 5, 6, and data not shown) (Newman and Krieg, 2002). Examination of sagittal sections shows that depletion of Wee2 caused an increase in the number of mitotic nuclei in the paraxial mesoderm by stage 18 of development (compare panels 1 and 2). This change in the mitotic index led to an increased total number of paraxial mesoderm cells, particularly in the posterior regions of the embryo (bracket, panel 6), but no increase in the number of axial mesoderm cells. Quantification of every sagittal and transverse section from representative CMO- and W2MO.1-treated embryos indicates that there was an 80% increase in the total number of nuclei found in the paraxial mesoderm of Wee2-depleted embryos (Fig. 2E). Conversely, there was no significant change in the number of nuclei found in the axial mesoderm of Wee2-depleted embryos. Despite the increase in the number of paraxial mesoderm cells, there was no change in the total volume of MyoD-expressing tissue (Fig. 2F). Together, these results indicate that Wee2 expression is required to maintain the low mitotic index of the paraxial mesoderm during neurulation. Furthermore, while the number of paraxial mesoderm cells increases in Wee2-depleted embryos, the size of the paraxial mesoderm remains unchanged.

Knockdown of Wee2 disrupts embryo elongation, somite formation and convergent extension

We next investigated the developmental consequences of depleting Wee2. Embryos were microinjected with W2MO.1, W2MO.2 or CMO, or left non-injected (sibling). These were allowed to develop for various periods of time before being processed for MyoD in situ analysis. Embryos depleted of Wee2 underwent cleavage and gastrulation normally, suggesting that Wee2 is not required for these early developmental stages (data not shown). However, as development continued, numerous defects became apparent. By stage 25 of development, sibling and CMO-treated embryos had developed an elongated, tadpole-like shape and each had ~15 somites (Fig. 3A, panels 1 and 2). By contrast, the Wee2 morpholino-treated embryos failed to elongate completely along their anteroposterior axis and failed to develop defined somites (panels 3 and 4). Although both of the Wee2-targeted morpholinos gave this phenotype in a high percentage of embryos, (W2MO.1, 85%, *n*=35; W2MO.2, 87%, *n*=32), this

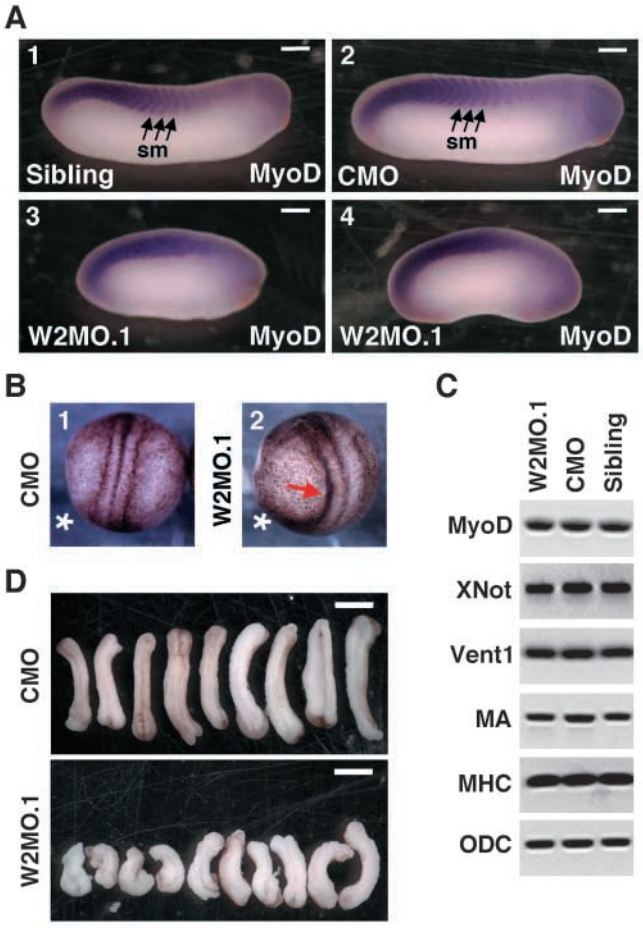

Fig. 3. Wee2 is required for anterior-posterior embryo elongation, somite formation, and convergent extension. (A) Wee2-depleted embryos fail to extend along the anteroposterior axis and fail to form somites. Embryos were treated as in Fig. 2D, but allowed to develop until the controls reached stage 25 before being processed for MyoD in situ analysis. Anterior towards the right, dorsal towards the top. Labels as in Fig. 1A. Scale bar: 300 μm. (B) Unilateral depletion of Wee2. One blastomere (asterisk) of a two-cell embryos was microinjected with 40 ng CMO or W2MO.1. These were allowed to develop until controls reached stage 19 and photographed. Dorsal view, anterior towards the top. Note curvature and reduced somitic ridge (arrow) on the Wee2-depleted side. (C) Mesoderm specific gene expression is unchanged in Wee2-depleted embryos. Quantitative RT-PCR for MyoD, XNot, Vent1, MA, MHC and ornithine decarboxylase (ODC) from whole, stage 18 embryos treated with W2MO.1, CMO or nothing (Sibling). (D) Depletion of Wee2 compromises convergent extension driven elongation of dorsal explants. Embryos were treated with W2MO.1 or CMO as in Fig. 2D and then processed for dorsal explants. Explants were photographed when controls reached stage 26. Scale bar: 1 mm.

phenotype was never observed in embryos treated with CMO. Using one half or one quarter as much Wee2 morpholino caused a less severe foreshortening of the embryo, but the percentage of embryos affected remained as high (data not shown). Embryos treated with the dose of Wee2 morpholino used in Fig. 3A (80 ng) died by the tailbud stage (stage 28), while embryos treated with the same amount of CMO continued to grow (*n*=28, 75%). This suggests that the loss of

Wee2 may be embryonic lethal. As might be expected from the protein depletion data (Fig. 2), the short, somite-deficient phenotype was slightly stronger with W2MO.1 than with W2MO.2 (Fig. 3A, panels 3 and 4). Because the in vitro and in vivo reduction of Wee2 protein and the in vivo phenotype were more pronounced with W2MO.1, we used it for the remainder of this study.

Although the lack of defined somites was readily apparent by stage 25 (Fig. 3A), we had observed this defect earlier in sagittal sections of stage 18 embryos (Fig. 2D). By stage 18 of development, normal *Xenopus* embryos are nearing the end of neurulation and have formed 2-3 somites. These somites are observed in CMO-treated embryos (Fig. 2D, arrows, panels 3 and 5), but are absent in embryos treated with W2MO.1 (Fig. 2D, panels 4 and 6). This led us to investigate whether the embryo foreshortening was also taking place earlier in development. The first cleavage in *Xenopus* development bisects the left and right halves of the embryo. This makes it is possible to uncouple the development of the two halves by treating only one blastomere (Sive et al., 2000). Either CMO or W2MO.1 were microinjected into the left blastomere (asterisk) of two-cell embryos and these embryos were allowed to develop until the controls were at stage 19 (Fig. 3B). Embryos unilaterally treated with W2MO.1 curved to the injected side (arrow), while the control treated embryos remained straight. This suggests that the side depleted of Wee2 cannot elongate as well as the control-injected side. The curvature defect was observed as early as mid-neurulation (data not shown) and was readily apparent in 80% of the embryos (n=15) by late neurulation (stage 19). Taken together, these results show that Wee2 depletion prevents proper formation of the somites and complete elongation of the embryo along its anteroposterior axis.

A priori, the reduced embryo elongation could be caused by a defect in mesoderm specific gene expression (Kopan et al., 1994) or by a defect in convergent extension (Keller, 2002; Wallingford et al., 2002). We investigated each of these possibilities. First, we compared the levels of various developmentally regulated mRNAs in CMO- and W2MO.1-treated whole embryos. We observed no difference in the level of axial (XNot), paraxial (MyoD) or ventral (Vent1) mesoderm markers (Dosch et al., 1997; Gawantka et al., 1995; von Dassow et al., 1993) suggesting that the early determination of these tissues remains intact in Wee2-depleted embryos (Fig. 3C). Furthermore, the early differentiation of paraxial mesoderm into muscle tissue appears normal in Wee2-depleted embryos, as judged by the expression of muscle actin (MA) and myosin heavy chain (MHC) (Mohun et al., 1988; Radice and Malacinski, 1989) (Fig. 3C). We next directly examined convergent extension by comparing the ability of dorsal explants from CMO (n=21) or W2MO.1 (n=18)-treated embryos to extend in vitro (Wilson et al., 1989). When Wee2 protein levels were reduced, the dorsal explants extended to only 65% of the length (on average) of control treated embryos (Fig. 3D). Conversely, injection of the control morpholino had no effect on explant extension compared with sibling controls (data not shown). Together, these results indicate that the reduced elongation observed in Wee2-depleted embryos is caused by a defect in some aspect of convergent extension. Furthermore, these results suggest that despite this convergent extension defect, the determination of the mesoderm and early differentiation of the paraxial mesoderm remain normal, at least through late neurulation, as judged by expression of specific markers.

Wee2 is required for neurulation-stage convergent extension of the paraxial mesoderm

To examine the convergent extension defect in more detail, we used markers specific to the axial mesoderm (XNot), paraxial mesoderm (MyoD, MA, MHC) and neuronal tissues (Sox3), to determine whether the developmental patterning and convergent extension of these tissues were affected by Wee2 depletion in the intact embryo (Dosch et al., 1997; Mohun et al., 1988; Radice and Malacinski, 1989; von Dassow et al., 1993; Zygar et al., 1998). Depletion of Wee2 had no effect on when gastrulation was initiated or completed, as measured by the formation of the dorsal lip and closure of the blastopore, respectively (data not shown). In addition, by the end of gastrulation (stage 13), dorsal views show that Wee2-depleted embryos appeared normal except for a slight mediolateral widening of the axial and paraxial mesoderm (Fig. 4A,B, panels 1 and 2 each). Thus, through the end of gastrulation, tissue rearrangements and convergent extension of the axial and paraxial mesoderm are relatively unaffected by Wee2 depletion.

The axial mesoderm continues to develop normally in Wee2-depleted embryos. By late neurulation, XNot has a normal pattern of expression and the notochord appears fully elongated (Fig. 4B, panels 3 and 4). The only noticeable defect is that the notochord is more readily visible on the dorsal surface of Wee2-depleted embryos (82% n=17). Bisection of XNot stained embryos indicates that this is because the notochord is not internalized completely or covered by the neural folds in Wee2 depleted embryos (data not shown). Together, these results indicate that depletion of Wee2 has little affect on the patterning and convergent extension of the axial mesoderm during gastrulation or neurulation.

The same is not true for the paraxial mesoderm. Although the gastrula stage movements were normal, defects in the positioning of the paraxial mesoderm were apparent by mid-neurulation in Wee2 depleted embryos (77%, n=18). Dorsal views of stage 15 embryos show that the paraxial mesoderm failed to complete its anterior and medial migration (Fig. 4A, compare panels 3 and 4). As neurulation continued (stage 18), the paraxial mesoderm migration defect became more obvious (70%, n=17). Dorsal and lateral views show that the paraxial mesoderm failed to complete its migration towards the midline or extension along the anteroposterior axis (Fig. 4A, compare panels 5 and 6, and 7 and 8). In addition, anterior views show that the ridge of presomitic mesoderm failed to form (yellow arrow) and that the neural folds failed to close (white arrow) (Fig. 4A, compare panels 9 and 10). These defects in paraxial mesoderm migration were also observed with the other Wee2 morpholino (W2MO.2, data not shown). Although depletion of Wee2 disrupted the migration of the paraxial mesoderm, it had little effect on muscle differentiation, as determined by the expression of muscle actin (MA) or myosin heavy chain (MHC), early and mid-stage differentiated muscle markers respectively (Chanoine and Hardy, 2003). As with MyoD, these genes are expressed normally, but their spatial distribution is disrupted (Fig. 3C, Fig. 4C).

The patterning defect of the paraxial mesoderm suggests that

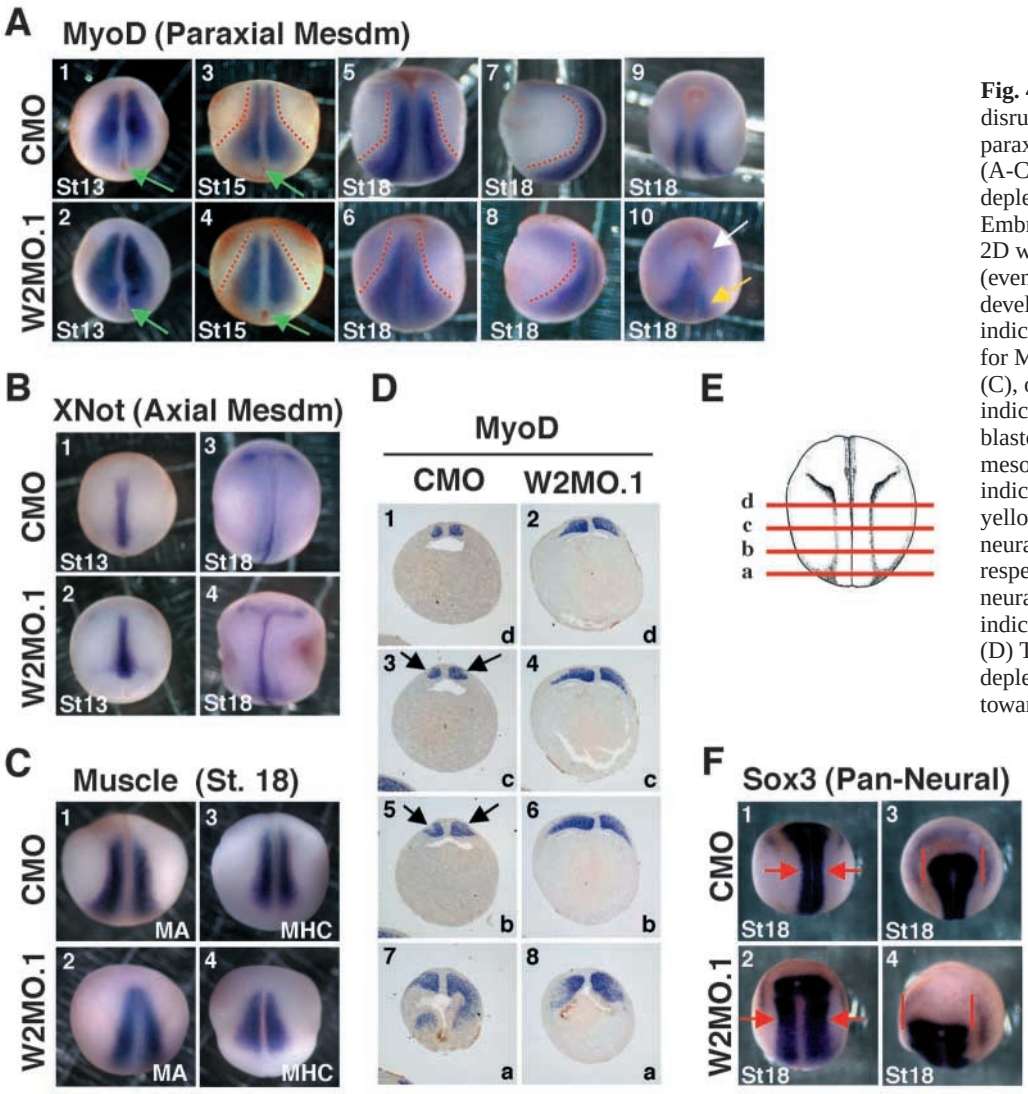

Fig. 4. Depletion of Wee2 protein disrupts convergent extension of the paraxial mesoderm during neurulation. (A-C,F) Temporal analysis of Wee2-depleted embryos during neurulation. Embryos were microinjected as in Fig. 2D with CMO (odd panels) or W2MO.1 (even panels), and were allowed to develop until controls reached the indicated stages before being processed for MyoD (A), XNot (B), MA and MHC (C), or Sox3 (F) in situ analysis as indicated. Green arrows indicate a closed blastopore. Lateral limits of paraxial mesoderm (MyoD expression) are indicated by broken red lines. White and yellow arrows indicate lack of anterior neural fold and somitic ridge, respectively. Lateral limits of presumptive neural tissue (Sox3 expression) are indicated by red arrows and vertical lines. (D) The paraxial mesoderm of Wee2-depleted embryos fails to converge towards the midline. Representative CMO and W2MO.1 treated, MyoD stained, stage 18 embryos from 4A were serially sectioned transversely. The anteroposterior positions of the shown sections are indicated by letters in right lower corner of panels as per E. Dorsal is towards the top. Black arrow indicates the forming somitic ridge. (E) Drawing reproduced, with permission, from Nieuwkoop and Faber (Nieuwkoop and Faber, 1994) showing position of cuts in D.

neurula-stage convergent extension of this tissue might be disrupted (Keller et al., 2000; Wallingford and Harland, 2001). To study this further, we examined a series of anterior to posterior transverse sections from late neurula-stage embryos that had been stained with the paraxial mesoderm marker MyoD after morpholino treatment. Depletion of Wee2 had profound effects on the positioning of the paraxial mesoderm. Unlike the controls, the paraxial mesoderm failed to migrate toward the midline in W2MO.1-treated embryos (Fig. 4D, compare panels 1, 3, 5 with 2, 4, 6). Normally, this movement leads to the dorsoventral thickening of paraxial mesoderm and the formation of the somitic ridge (arrows in controls). Both of these events are blocked in Wee2-depleted embryos. In addition, W2MO.1-treated embryos lack the normal posterior extension of the paraxial mesoderm around the blastopore (Fig. 4D, compare panels 7 and 8).

Finally, we examined the patterning of the neural plate in late neurula stage embryos using Sox3 as a pan-neuronal marker (Fig. 4F). In Wee2-depleted embryos, the neural plate fails to migrate toward the midline, form normal neural folds, or extend anteriorly completely (80%, n=10). This defect in neuronal patterning is unlikely to be a direct effect of Wee2 depletion, as Wee2 is not expressed in neural tissues during neurulation (Leise and Mueller, 2002). A likely scenario is that the defect in the convergent extension of the underlying paraxial mesoderm influences the migration of the overlaying neural plate (Keller et al., 2000). Although neuronal tissues have been shown to undergo convergent extension independently in explants, it has also been suggested that the complete migration of the neuronal tissue toward the midline depends on the underlying mesoderm in vivo. Finally, although the migration of the neural plate is disrupted in Wee2-depleted embryos, this tissue still differentiates as judged by the expression of N-tubulin (data not shown) (Hardcastle and Papalopulu, 2000). Together, these experiments show that neurula-stage convergent extension of the paraxial mesoderm is compromised when Wee2 protein levels are reduced.

Exogenous Wee2 can rescue the Wee2 depletion phenotype

An important control in morpholino-mediated depletions is the rescue of the induced phenotype. To accomplish this, we microinjected both blastomeres of two-cell embryos with various mixtures of constant amounts of W2MO.1 and

increasing amounts of Wee2 mRNA that lacks the morpholino target site. Subsequently, these embryos and non-injected siblings were raised to stage 19 and processed for MyoD or Sox3 in situ analysis (Fig. 5). As expected, microinjection of W2MO.1 with buffer alone recapitulated the defects observed previously (*n*=23, 89%). There was a lack of paraxial mesoderm convergent extension as marked by the lateral extension of MyoD and a lack of neural plate movement as marked by the lateral extension of Sox3 and the wide neural plate devoid of defined neural folds (compare panels 1-4 with 13-16). Embryos co-injected with as little as 20 pg of Wee2 mRNA showed a partial rescue of these defects (panels 5-8; *n*=53, 87%), while embryos co-injected with 40 pg of Wee2 mRNA appeared almost normal (panels 9-12; *n*=59, 64%). Attempts to completely rescue the phenotype failed because all embryos microinjected with just twofold more Wee2 mRNA (80 pg) died during gastrulation (data not shown). Furthermore, even the embryos that displayed partial rescue with lower amount of mRNA (panels 5-12), died shortly after controls completed neurulation. These early embryonic deaths were not totally unexpected because Wee2 is a potent cell cycle inhibitor and because expression of Wee2 throughout the embryo may be deleterious (Leise and Mueller, 2002). However, the partial rescue observed with moderate levels of Wee2 mRNA indicates that Wee2 is necessary for convergent extension of paraxial mesoderm.

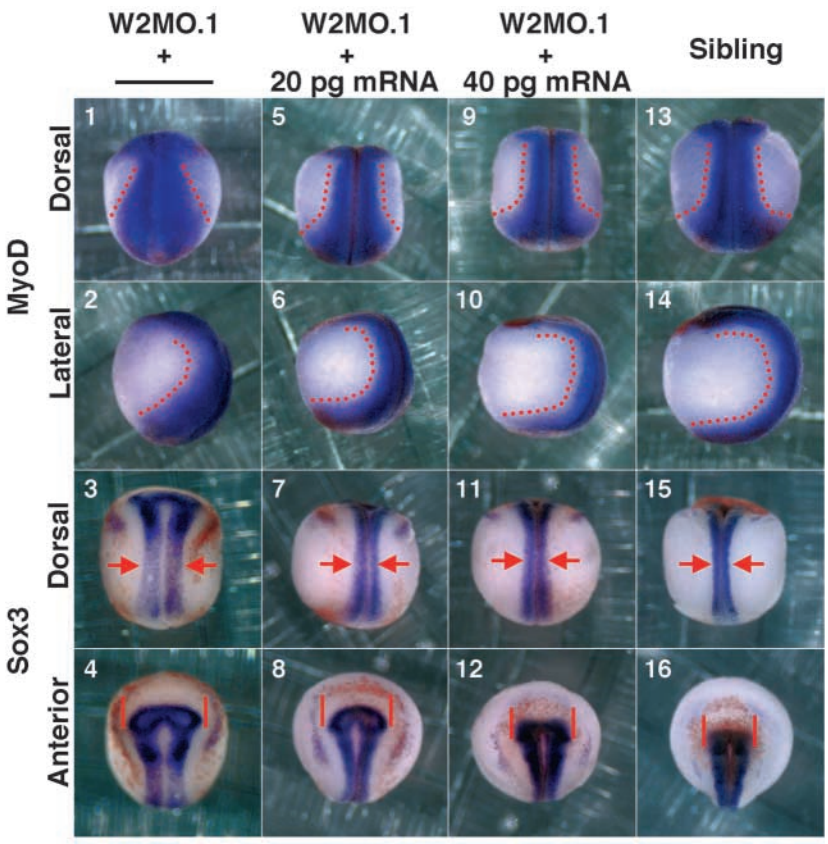

Fig. 5. Rescue of Wee2-depleted embryos. Both blastomeres of two-cell embryos were microinjected with a combination of 40 ng W2MO.1 and either injection buffer (panels 1-4), 20 pg Wee2 mRNA (panels 5-8) or 40 pg Wee2 (panels 9-12). These were allowed to develop until non-injected siblings (panels 13-16) reached stage 19. Subsequently, the embryos were subjected to MyoD or Sox3 in situ analysis as indicated. Lateral limits of paraxial mesoderm (MyoD expression) are indicated by broken red lines. Lateral limits of presumptive neural tissue (Sox3 expression) are indicated by red arrows and vertical lines.

Inhibition of the cell cycle is required for convergent extension of the paraxial mesoderm

Having established that Wee2 is required for convergent extension of the paraxial mesoderm during neurulation, we next asked whether this requirement was for cell cycle inhibition or for some other, unknown, function of Wee2. To accomplish this, we induced premature cell cycle progression by the ectopic expression of either a constitutively active Cdk or an active Cdc25 and then asked whether this led to a convergent extension defect. First we tested a constitutively active form of Cdk2, a Cdk that indirectly promotes the G2 to M phase transition in *Xenopus* (Guadagno and Newport, 1996). Cdk2 can be made constitutively active by mutation of the Thr14 and Tyr15 sites to non-phosphorylatable alanine and phenylalanine, respectively (Gu et al., 1992). We microinjected various amounts of either wild type (WT) or non-phosphorylatable (AF) Cdk2 into both blastomeres of two-cell embryos and analyzed the convergent extension of the mesoderm by monitoring the expression patterns of MyoD and XNot.

Embryos injected with 230 pg of Cdk2WT per blastomere developed normally (Fig. 6A, panels 1 and 3, 92%, *n*=26). By contrast, embryos injected with 230 pg of Cdk2AF displayed reduced mediolateral migration and reduced anteroposterior extension (convergent extension) of the paraxial mesoderm and failed to form proper neural folds (arrow) (panels 2 and 4, 80%, *n*=25). The defect in paraxial mesoderm convergent extension can be clearly observed in an anterior to posterior series of transverse sections from late neural stage embryos prepared for MyoD in situ analysis (Fig. 6B). Microinjection of Cdk2AF (right panels), but not Cdk2WT (left panels), blocks mediolateral convergence to the midline (compare panels 1, 3, 5 with 2, 4, 6), posterior extension around the blastopore (compare panels 7 and 8), and somitic ridge formation (arrows in Cdk2WT). Microinjection of AF or WT Cdk2 had little effect on the axial mesoderm, except that the notochord was not internalized in the Cdk2AF-injected embryos (85% *n*=20) (Fig. 6A, compare panels 5 and 6). Interestingly, expression of Cdk2AF led to a 40% increase in the number of paraxial mesoderm cells, but no significant change in the number of axial mesoderm cells (Fig. 6C). Although this is consistent with the tissue specificity of the convergent extension defect, it raises the possibility that a phosphorylation-independent mechanism is used to control Cdk2 activity and cell cycle arrest in the axial mesoderm.

As was observed with cell cycle advancement mediated by knockdown of Wee2, ectopic expression of Cdk2AF compromised convergent extension of dorsal explants in vitro, but had no detectable effect on the expression of mesodermal

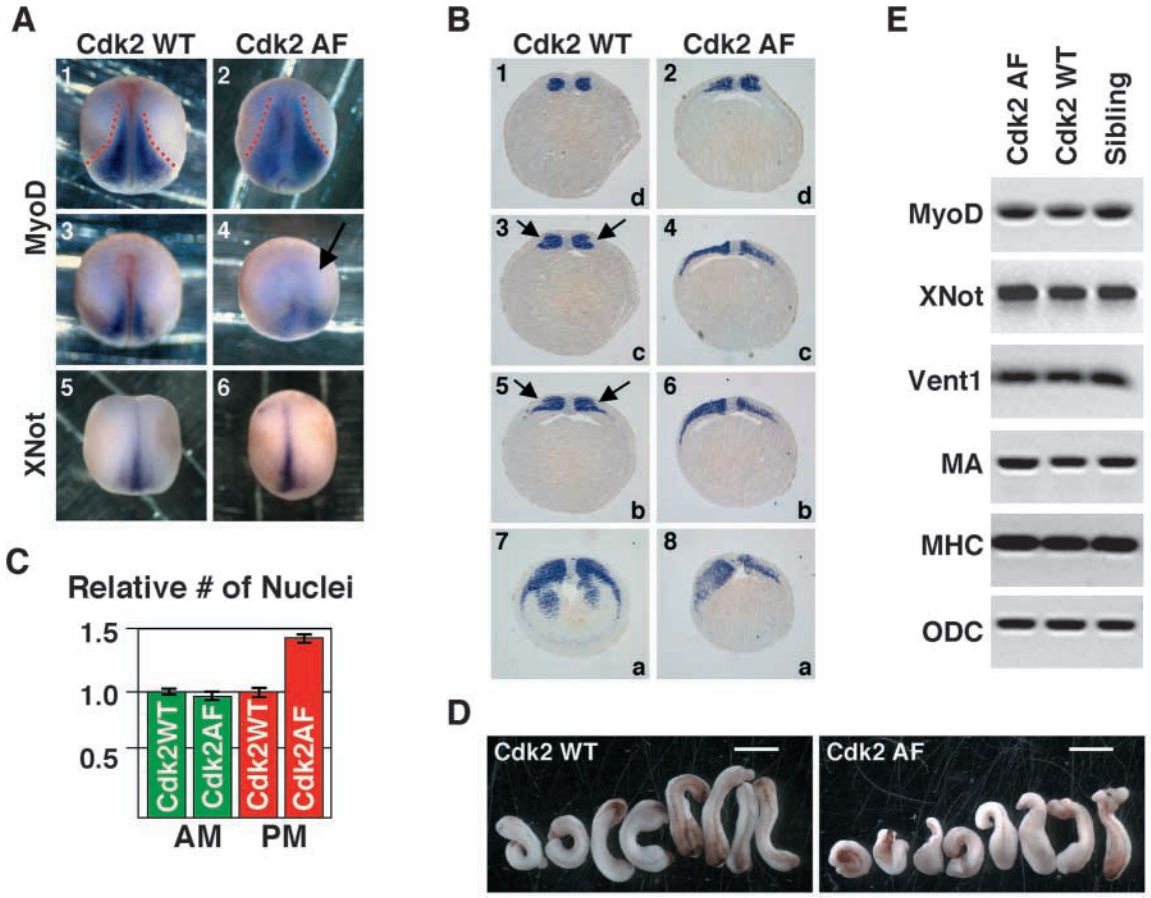

Fig. 6. Expression of constitutively active Cdk2 phenocopies the convergent extension defects observed in Wee2-depleted embryos. (A) Both blastomeres of two-cell embryos were microinjected with 230 pg of Cdk2WT or Cdk2AF mRNA as indicated. These embryos were allowed to develop until stage 18 before being processed for MyoD or XNot in situ analysis. Lateral limits of paraxial mesoderm (MyoD expression) are noted by broken lines. Arrow indicates lack of anterior neural fold. (B) The paraxial mesoderm of Cdk2 AF-treated embryos fails to converge towards the midline. Representative Cdk2WT or Cdk2AF treated, MyoD stained, stage 18 embryos from 6A were serially sectioned transversely. The anteroposterior positions of the shown sections are indicated by letters in right lower corner of panels as per Fig. 4E. Dorsal towards the top. Black arrow denotes the forming somitic ridge. (C) Expression of Cdk2AF causes cell proliferation within the paraxial mesoderm but not the axial mesoderm. The total number of nuclei within the paraxial and axial mesoderm of representative embryos from 6A was determined as in Fig. 2E. (D) Cdk2 AF treatment compromises convergent extension driven elongation of dorsal explants. Embryos were injected with Cdk2 WT or Cdk2 AF mRNA as in A and then processed for dorsal explants. Explants were photographed when controls reached stage 24. Scale bar: 1 mm. (E) Mesoderm specific gene expression is unchanged in Cdk2 AF-treated embryos. Quantitative RT-PCR for MyoD, XNot, Vent1, MA, MHC and ODC from whole, stage 18 embryos injected as in A with Cdk2 AF mRNA, Cdk2 WT mRNA, or nothing (Sibling).

genes in the intact embryo. Dorsal explants from Cdk2AF (n=11)-injected embryos extended to only 68% of the length (on average) of Cdk2WT (n=12) injected embryos (Fig. 6D). Conversely, we observed no difference in the level of MyoD, XNot, Vent1, MA and MHC suggesting that the early determination of the mesoderm and differentiation of the paraxial mesoderm are normal in Cdk2AF treated embryos (Fig. 6E). Thus, ectopic expression of constitutively active Cdk2 causes an increase in cell proliferation in the paraxial mesoderm and this leads to a convergent extension defect in the paraxial mesoderm without affecting early muscle differentiation.

As an alternative approach to promote premature cell cycle progression, we used a developmentally regulated promoter to mis-express Cdc25 specifically in differentiating muscle. The Cdc25 phosphatases are the antagonists of the Wee kinases (Morgan, 1997). Two Cdc25 phosphatases have been identified in *Xenopus*, Cdc25A and Cdc25C, and both have been shown to promote entry into mitosis in developing *Xenopus* embryos (Kim et al., 1999). We placed phosphatase-active (WT) and -dead (PD) versions of Cdc25A- and Cdc25C-GFP fusion constructs under the control of the cardiac actin promoter (Kroll and Amaya, 1996). This promoter has been shown to express exogenous genes in the paraxial mesoderm as this tissue differentiates into muscle (Mohun et al., 1989). Thus, transcripts begin to appear during mid-gastrulation, but high levels of expression in the paraxial mesoderm are not detected until neurulation. When injected as plasmid DNA, cells will express the construct in a largely tissue specific, but mosaic pattern, depending on whether the cell has passively inherited the DNA (Sive et al., 2000). In the first set of experiments, we microinjected 100 pg of the Cdc25A- or Cdc25C-GFP fusion plasmids into one blastomere of a two-cell embryo. These unilaterally treated embryos were allowed to develop until

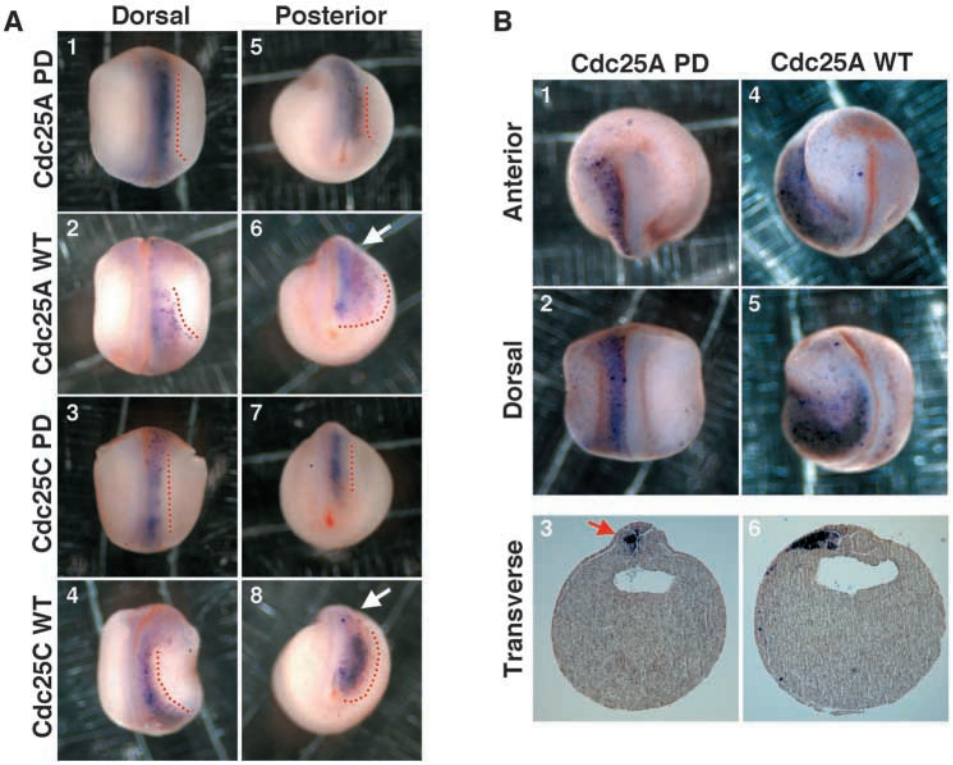

Fig. 7. Paraxial mesoderm targeted expression of wild-type Cdc25 disrupts convergent extension. (A) Dorsal and posterior views of embryos unilaterally injected with 100 pg of the indicated Cdc25 plasmid DNA. Embryos were allowed to develop until stage 19 before being processed for GFP in situ analysis. Cells expressing GFP-Cdc25 stain blue. WT [wild type (active)] and PD [phosphatase-dead (inactive)] forms of Cdc25A or Cdc25C. Lateral limits of GFP-Cdc25 positive cells are indicated by broken lines. Arrows indicate the lack of a somatic ridge. (B) Dorsal, anterior and sectioned views of embryos unilaterally injected and treated as in A, except 300 pg of Cdc25A plasmid DNA was used. Arrow indicates somitic ridge.

stage 19 before being processed for GFP in situ analysis to detect the position of Cdc25 expressing cells (Fig. 7A). Although cells that express the phosphatase-dead versions of either Cdc25 converge to the midline normally (odd numbered panels), many cells that express active versions of these phosphatases fail to do so (even numbered panels). In addition, cells expressing the active, but not dead, phosphatases fail to migrate anteriorly (compare panels 1 and 2, and 3 and 4). These defects appear to have global effects on the embryo in that the somitic ridge is improperly formed (arrow) on the injected side of most embryos expressing active Cdc25 (compare panels 5 and 6, and 7 and 8) and that the embryos curve towards the injected side in about half the cases (panel 4). These global defects were not observed with the phosphatase-dead constructs.

We observed a dose-dependent phenotype with Cdc25 plasmid microinjection. When three times as much Cdc25A was microinjected (300 pg), most of the cells of the paraxial mesoderm expressed the exogenous Cdc25A (Fig. 7B). The majority of the embryos injected with active Cdc25A curved towards the microinjected side as they failed to complete medial and anterior migration of the paraxial mesoderm (panels 4 and 5, 60% n=30). Similar results were observed when we microinjected active Cdc25C DNA (data not shown, 68% n=25). By contrast, embryos microinjected with 300 pg of phosphatase-dead Cdc25A (panels 1 and 2, 67% n=15) or phosphatase-dead Cdc25C (data not shown, 76% n=25) developed normally. The Cdc25A-treated embryos were analyzed further in transverse sections (panels 3 and 6). In both cases, Cdc25 was expressed in the paraxial mesoderm, but when Cdc25A is active, the paraxial mesoderm fails to converge toward the midline or to form a proper somitic ridge (arrow). These results suggest that mis-expression of active Cdc25A or Cdc25C in the paraxial mesoderm leads to the same developmental defects as loss of Wee2. Combined with the results observed with Wee2 depletion and Cdk2AF expression, these results indicate that cell cycle arrest during neurulation is required for convergent extension of the paraxial mesoderm.

Discussion

We are interested in understanding the molecular mechanisms that coordinate cell cycle regulation with the critical morphogenetic movements that shape the developing vertebrate embryo. Both cell division and cell migration are needed during early development. However, these events use a common pool of cytoskeletal elements and require opposing levels of cell adhesion. Thus, the occurrence of cell proliferation and cell rearrangement must be temporally coordinated during development. The need for this coordination is particularly true in the case of integrated cell movements such as convergent extension, involution and invagination. During these complex morphogenetic movements, cells behave and migrate not as individuals, but as integral parts of a whole tissue (Keller, 2002; Wallingford et al., 2002). The cells must change shape and adopt a polarized morphology while remaining adherent to the extracellular matrix and/or to each other (Keller et al., 2000). These cellular states are incompatible with mitosis, the last phase in the cell cycle, where cells commonly round up and lose adherence to their substrate. In this study, we have found that convergent extension of the paraxial mesoderm in *Xenopus* requires an arrest in the cell cycle and that this arrest is dependent on a potent mitotic inhibitor, Wee2.

Cell divisions are rapid and synchronous during early development in *Xenopus*. However, the rate of these divisions

slows and becomes spatially restricted with the onset of gastrulation (Masui and Wang, 1998). In particular, the cells of the paraxial mesoderm stop dividing as this tissue undergoes the concerted cell movement of convergent extension. Eventually, the cells of the paraxial mesoderm re-enter the cell cycle as they form significant parts of the muscle, skeletal and dermal elements of the embryo. Wee2, one of three Cdk inhibitory kinases found in vertebrates, is expressed in the paraxial mesoderm from mid-gastrulation onwards. Like other Wee kinases, Wee2 inhibits Cdk activity by phosphorylating a conserved tyrosine residue in the active site of the Cdk, and therefore prevents entry into mitosis (Leise and Mueller, 2002). In this work, we have shown that Wee2 plays a causative role in the low mitotic index of the paraxial mesoderm as depletion of the Wee2 protein increases the proliferation of this tissue during neurulation. As might be expected, tissues that do not express Wee2 show no change in their normal mitotic index with the depletion of Wee2.

The absence of cell proliferation in the paraxial mesoderm is important for normal development. Embryos bilaterally depleted of Wee2 fail to elongate completely, while embryos unilaterally depleted of Wee2 curve towards the depleted side. These elongation and curvature defects are the result of aberrant convergent extension of the paraxial mesoderm during neurulation. Because of the lack of convergent extension, the somitic ridge fails to form and the neural plate fails to move toward the midline. The occurrence of these defects is not limited to the morpholino-mediated depletion of Wee2, but can be phenocopied by other manipulations that cause premature advancement in the cell cycle. These include the mis-expression of wild-type forms of Cdc25 and non-phosphorylatable forms of Cdk2. Finally, Wee2-depleted embryos fail to undergo somitogenesis. However, because somitogenesis is a late event during neurulation, our results do not allow us to resolve whether the absence of somitogenesis is a direct effect of Wee2 depletion or the result of prior inhibition of convergent extension and positioning of the paraxial mesoderm.

In contrast to the deficiencies in convergent extension of the paraxial mesoderm, other morphogenetic movements appear to be intact in Wee2-depleted embryos. Gastrula stage cell movements such as involution of the mesoderm and closure of the blastopore are initiated and completed on schedule. In addition, the axial mesoderm (notochord) appears to extend and develop normally during neurulation. Finally, as expected, we do not see the extreme phenotype that is observed when the PCP pathway is globally disrupted in the intact embryo. As the PCP pathway controls convergent extension in three tissues, the axial mesoderm, the paraxial mesoderm and the neural tissue, global disruption of this pathway results in embryos that are not only foreshortened but also that have incomplete closure of the neural folds and extreme dorsal flexure (Sokol, 1996; Tada and Smith, 2000; Wallingford and Harland, 2001; Wallingford et al., 2000). In Wee2-depleted embryos, only the paraxial mesoderm was affected.

Other developmental events also appear to be intact in Wee2-depleted embryos. For example, the continued expression of mesoderm markers MyoD, XNot and Vent1 suggests that the fate of the paraxial, axial and ventral mesoderm cells remain unchanged. Furthermore, the expression of muscle actin (MA) and myosin heavy chain (MHC) suggests that early myogenic differentiation is unperturbed (Chanoine and Hardy, 2003). Finally, neuronal induction and differentiation appear relatively normal as judged by the expression of the pan-neuronal maker Sox3 and the neuronal differentiation marker N-tubulin (data not shown) (Hardcastle and Papalopulu, 2000). Thus, the need for Wee2-mediated control of the cell cycle during the neurulation stage of development is limited to processes that permit orchestrated cell movement and patterning of the paraxial mesoderm.

During *Drosophila* gastrulation, a similar cell cycle arrest is observed in the ventral mesoderm as it undergoes invagination and ventral furrow formation (Foe, 1989). As with the paraxial mesoderm of *Xenopus*, this block is transient; once the ventral mesoderm cells of *Drosophila* have completed invagination, they re-enter the cell cycle. In wild-type flies, the ventral mesoderm cells are arrested due to the expression of Tribbles, a gene product that promotes the proteolysis of Cdc25 (Großhans and Wieschaus, 2000; Mata et al., 2000; Seher and Leptin, 2000). As Cdc25 is the antagonist of Wee2, degradation of Cdc25 has the same effect as expression of Wee2, namely the maintenance of Cdks in their inhibited, phosphorylated state. In fact, forced cell cycle advancement induced by the mis-expression of Cdc25 or by the loss of Tribbles blocks the rapid invagination of the ventral mesoderm in flies (Edgar and O'Farrell, 1990; Großhans and Wieschaus, 2000; Mata et al., 2000; Seher and Leptin, 2000). Thus, at least two types of integrated cell movements, convergent extension of the paraxial mesoderm in *Xenopus* and invagination of the ventral mesoderm cells in *Drosophila*, use inhibitory phosphorylation of the Cdks to prevent cell division during these movements.

Although cell cycle arrest is important in some cases of integrated cell movement, it is not an absolute or universal requirement for cell migration. For example, although the ventral mesoderm of Tribbles mutants undergoes inappropriate cell division, this tissue eventually migrates into the embryo (Mata et al., 2000; Seher and Leptin, 2000). However, this movement is slow, as well as disorganized, and causes a majority of the Tribbles mutants to die during embryogenesis. Thus, Tribbles ensures that the cell movement is rapid and coordinated. In a second example, cell cycle arrest may not be essential for movement of the presumptive neuronal tissue of *Xenopus*. Like the mesoderm, the neural ectoderm undergoes convergence and extension during neurulation. However, unlike the mesoderm, at least part of this tissue is proliferating during this process (Hartenstein, 1989). This might partly explain why the force generated by convergent extension of the neuronal tissue is less than that of the underlying mesoderm (Keller et al., 2000). Together, these examples suggest that integrated cell movements may not so much need cell cycle arrest, as function more efficiently and rapidly when cell division is prevented. Still, in the cases of convergent extension of the paraxial mesoderm or ventral furrow formation, cell cycle arrest is required for normal development.

As Wee2 is expressed in the paraxial mesoderm from mid-gastrulation onwards, it is not surprising that morpholino-mediated depletion of Wee2 only disrupts events after the completion of gastrulation. However, this raises the question of what causes the cell cycle arrest of the paraxial mesoderm earlier during gastrulation and the cell cycle arrest of the axial mesoderm throughout gastrulation and neurulation. One possible candidate is the maternally expressed Wee1, a kinase

related to Wee2 (Mueller et al., 1995a). Although Wee1 mRNA disappears during gastrulation, Wee1 protein is present through neurulation (Murakami and Vande Woude, 1998) (data not shown). This stable pool of Wee1 protein might block the cell cycle in these tissues. Alternatively, maternally expressed Myt1 (another Cdk inhibitory kinase) may contribute to this arrest (Mueller et al., 1995b). Finally, mechanisms independent of inhibitory Cdk phosphorylation may be involved. A likely candidate is p27Xic1, the only Cdk binding inhibitor found to date in *Xenopus*. However, in this context, it is interesting that whereas depletion of p27Xic1 profoundly perturbed differentiation of muscle and neuronal tissues, it did not appear to effect convergent extension (Carruthers et al., 2003; Vernon et al., 2003; Vernon and Philpott, 2003). Thus, although our results implicate Wee2 as the major mediator of cell cycle arrest in paraxial mesoderm during neurulation, they do not rule out contributions by other cell cycle inhibitors.

In conclusion, we have shown that Wee2 coordinates cell cycle regulation with critical morphogenetic movements. Wee2 is required both to prevent cell division and to allow the complete convergent extension and somitogenesis of the paraxial mesoderm during neurulation. Our results suggest that convergent extension and cell division are incompatible in the paraxial mesoderm of *Xenopus*. By arresting the cell cycle, Wee2 prevents the morphological catastrophe that results from tissues trying to carry out these processes simultaneously.

We thank members of the Mueller laboratory, Drs A. Bruce, E. Ferguson, J. Malamy, A. Oates, V. Prince, T. Sosnick and T. Steck for their helpful comments on this work and critical reading of this manuscript. We thank Dr R. Keller for helpful advice on the dorsal explants; and Drs. J. Gautier, D. Kimelman, K. Kroll, A. MacNicol, J. Maller, S. Moody, D. Morgan, C. Niehrs, A. Philpott and D. Turner for gifts of reagents; and S. Adawy, J. Coralic and R. Relwani for technical assistance. This work was supported by a grant to P.R.M. from the National Institutes of Health (RO1 CA84007).

References

Agius, E., Oelgeschlager, M., Wessely, O., Kemp, C. and de Robertis, E. M. (2000). Endodermal Nodal-related signals and mesoderm induction in Xenopus. *Development* **127**, 1173-1183.

Anderson, J. A., Lewellyn, A. L. and Maller, J. L. (1997). Ionizing radiation induces apoptosis and elevates cyclin A1-Cdk2 activity before but not after the midblastula transition in Xenopus. *Mol. Biol. Cell* **8**, 1195-1206.

Carruthers, S., Mason, J. and Papalopulu, N. (2003). Depletion of the cell-cycle inhibitor p27(Xic1) impairs neuronal differentiation and increases the number of ElrC(+) progenitor cells in Xenopus tropicalis. *Mech. Dev.* **120**, 607-616.

Chanoine, C. and Hardy, S. (2003). Xenopus muscle development: from primary to secondary myogenesis. *Dev. Dyn.* **226**, 12-23.

Cooke, J. (1973). Properties of the primary organization field in the embryo of Xenopus laevis. IV. Pattern formation and regulation following early inhibition of mitosis. *J. Embryol. Exp. Morphol.* **30**, 49-62.

Cooke, J. (1979). Cell number in relation to primary pattern formation in the embryo of Xenopus laevis. II. Sequential cell recruitment, and control of the cell cycle, during mesoderm formation. *J. Embryol. Exp. Morphol.* **53**, 269-289.

Costanzo, V., Robertson, K., Ying, C. Y., Kim, E., Avvedimento, E., Gottesman, M., Grieco, D. and Gautier, J. (2000). Reconstitution of an ATM-dependent checkpoint that inhibits chromosomal DNA replication following DNA damage. *Mol. Cell* **6**, 649-659.

Dosch, R., Gawantka, V., Delius, H., Blumenstock, C. and Niehrs, C. (1997). Bmp-4 acts as a morphogen in dorsoventral mesoderm patterning in Xenopus. *Development* **124**, 2325-2334.

Edgar, B. A. and O'Farrell, P. H. (1990). The three postblastoderm cell cycles of Drosophila embryogenesis are regulated in G2 by string. *Cell* **62**, 469-480.

Foe, V. E. (1989). Mitotic domains reveal early commitment of cells in Drosophila embryos. *Development* **107**, 1-22.

Gawantka, V., Delius, H., Hirschfeld, K., Blumenstock, C. and Niehrs, C. (1995). Antagonizing the Spemann organizer: role of the homeobox gene Xvent-1. *EMBO J.* **14**, 6268-6279.

Gont, L. K., Steinbeisser, H., Blumberg, B. and de Robertis, E. M. (1993). Tail formation as a continuation of gastrulation: the multiple cell populations of the Xenopus tailbud derive from the late blastopore lip. *Development* **119**, 991-1004.

Großhans, J. and Wieschaus, E. (2000). A genetic link between morphogenesis and cell division during formation of the ventral furrow in Drosophila. *Cell* **101**, 523-531.

Gu, Y., Rosenblatt, J. and Morgan, D. O. (1992). Cell cycle regulation of CDK2 activity by phosphorylation of Thr160 and Tyr15. *EMBO J.* **11**, 3995-4005.

Guadagno, T. M. and Newport, J. W. (1996). Cdk2 kinase is required for entry into mitosis as a positive regulator of Cdc2-cyclin B kinase activity. *Cell* **84**, 73-82.

Hardcastle, Z. and Papalopulu, N. (2000). Distinct effects of XBF-1 in regulating the cell cycle inhibitor p27(XIC1) and imparting a neural fate. *Development* **127**, 1303-1314.

Harris, W. A. and Hartenstein, V. (1991). Neuronal determination without cell division in Xenopus embryos. *Neuron* **6**, 499-515.

Hartenstein, V. (1989). Early neurogenesis in Xenopus: the spatio-temporal pattern of proliferation and cell lineages in the embryonic spinal cord. *Neuron* **3**, 399-411.

Hartley, R. S., Rempel, R. E. and Maller, J. L. (1996). In vivo regulation of the early embryonic cell cycle in Xenopus. *Dev. Biol.* **173**, 408-419.

Heasman, J. (2002). Morpholino oligos: making sense of antisense? *Dev. Biol.* **243**, 209-214.

Hopwood, N. D., Pluck, A. and Gurdon, J. B. (1989). MyoD expression in the forming somites is an early response to mesoderm induction in Xenopus embryos. *EMBO J.* **8**, 3409-3417.

Keller, R. (2002). Shaping the vertebrate body plan by polarized embryonic cell movements. *Science* **298**, 1950-1954.

Keller, R., Davidson, L., Edlund, A., Elul, T., Ezin, M., Shook, D. and Skoglund, P. (2000). Mechanisms of convergence and extension by cell intercalation. *Philos. Trans. R. Soc. Lond. B Biol. Sci.* **355**, 897-922.

Kim, S. H., Li, C. and Maller, J. L. (1999). A maternal form of the phosphatase Cdc25A regulates early embryonic cell cycles in Xenopus laevis. *Dev. Biol.* **212**, 381-391.

Kopan, R., Nye, J. S. and Weintraub, H. (1994). The intracellular domain of mouse Notch: a constitutively activated repressor of myogenesis directed at the basic helix-loop-helix region of MyoD. *Development* **120**, 2385-2396.

Kroll, K. L. and Amaya, E. (1996). Transgenic Xenopus embryos from sperm nuclear transplantations reveal FGF signaling requirements during gastrulation. *Development* **122**, 3173-3183.

Leise, W., 3rd and Mueller, P. R. (2002). Multiple Cdk1 inhibitory kinases regulate the cell cycle during development. *Dev. Biol.* **249**, 156-173.

MacNicol, M. C., Pot, D. and MacNicol, A. M. (1997). pXen, a utility vector for the expression of GST-fusion proteins in Xenopus laevis oocytes and embryos. *Gene* **196**, 25-29.

Masui, Y. and Wang, P. (1998). Cell cycle transition in early embryonic development of Xenopus laevis. *Biol. Cell* **90**, 537-548.

Mata, J., Curado, S., Ephrussi, A. and Rorth, P. (2000). Tribbles coordinates mitosis and morphogenesis in Drosophila by regulating string/CDC25 proteolysis. *Cell* **101**, 511-522.

Mohun, T., Garrett, N., Stutz, F. and Sophr, G. (1988). A third striated muscle actin gene is expressed during early development in the amphibian Xenopus laevis. *J. Mol. Biol.* **202**, 67-76.

Mohun, T. J., Taylor, M. V., Garrett, N. and Gurdon, J. B. (1989). The CArG promoter sequence is necessary for muscle-specific transcription of the cardiac actin gene in Xenopus embryos. *EMBO J.* **8**, 1153-1161.

Morgan, D. O. (1997). Cyclin-dependent kinases: engines, clocks, and microprocessors. *Annu. Rev. Cell Dev. Biol.* **13**, 261-291.

Mueller, P. R., Coleman, T. R. and Dunphy, W. G. (1995a). Cell cycle regulation of a Xenopus Wee1-like kinase. *Mol. Biol. Cell* **6**, 119-134.

Mueller, P. R., Coleman, T. R., Kumagai, A. and Dunphy, W. G. (1995b). Myt1: a membrane-associated inhibitory kinase that phosphorylates Cdc2 on both threonine-14 and tyrosine-15. *Science* **270**, 86-90.

Murakami, M. S. and Vande Woude, G. F. (1998). Analysis of the early

embryonic cell cycles of Xenopus; regulation of cell cycle length by Xe-wee1 and Mos. *Development* **125**, 237-248.

Myers, D. C., Sepich, D. S. and Solnica-Krezel, L. (2002). Convergence and extension in vertebrate gastrulae: cell movements according to or in search of identity? *Trends Genet.* **18**, 447-455.

Newman, C. S. and Krieg, P. A. (2002). Xenopus bagpipe-related gene, koza, may play a role in regulation of cell proliferation. *Dev. Dyn.* **225**, 571-580.

Nieuwkoop, P. D. and Faber, J. (1994). *Normal Table of* Xenopus Laevis *(Daudin)*. New York: Garland Publishing.

Radice, G. P. and Malacinski, G. M. (1989). Expression of myosin heavy chain transcripts during Xenopus laevis development. *Dev. Biol.* **133**, 562-568.

Saka, Y. and Smith, J. C. (2001). Spatial and temporal patterns of cell division during early Xenopus embryogenesis. *Dev. Biol.* **229**, 307-318.

Sater, A. K., Steinhardt, R. A. and Keller, R. (1993). Induction of neuronal differentiation by planar signals in Xenopus embryos. *Dev. Dyn.* **197**, 268-280.

Seher, T. C. and Leptin, M. (2000). Tribbles, a cell-cycle brake that coordinates proliferation and morphogenesis during Drosophila gastrulation. *Curr. Biol.* **10**, 623-629.

Sive, H. L., Grainger, R. M. and Harland, R. M. (2000). *Early Development of* Xenopus laevis: *A Laboratory Manual*. Cold Spring Harbor: Cold Spring Harbor Press.

Sokol, S. Y. (1996). Analysis of Dishevelled signalling pathways during Xenopus development. *Curr. Biol.* **6**, 1456-1467.

Steinbach, O. C. and Rupp, R. A. W. (1999). Quantitative analysis of mRNA levels in *Xenopus* embryos by reverse transcriptase-polymerase chain reaction (RT-PCR). In *Molecular Methods in Developmental Biology:* Xenopus *and Zebrafish*, Vol. 127 (ed. M. Guille), pp. 41-56. Totowa, NJ: Humana Press.

Stutz, F. and Spohr, G. (1986). Isolation and characterization of sarcomeric actin genes expressed in Xenopus laevis embryos. *J. Mol. Biol.* **187**, 349-361.

Tada, M. and Smith, J. C. (2000). Xwnt11 is a target of Xenopus Brachyury: regulation of gastrulation movements via Dishevelled, but not through the canonical Wnt pathway. *Development* **127**, 2227-2238.

Turner, D. L. and Weintraub, H. (1994). Expression of achaete-scute homolog 3 in Xenopus embryos converts ectodermal cells to a neural fate. *Genes Dev.* **8**, 1434-1447.

Vernon, A. E. and Philpott, A. (2003). A single cdk inhibitor, p27Xic1, functions beyond cell cycle regulation to promote muscle differentiation in Xenopus. *Development* **130**, 71-83.

Vernon, A. E., Devine, C. and Philpott, A. (2003). The cdk inhibitor p27Xic1 is required for differentiation of primary neurones in Xenopus. *Development* **130**, 85-92.

Vidwans, S. J. and Su, T. T. (2001). Cycling through development in Drosophila and other metazoa. *Nat. Cell Biol*. **3**, E35-E39.

von Dassow, G., Schmidt, J. E. and Kimelman, D. (1993). Induction of the Xenopus organizer: expression and regulation of Xnot, a novel FGF and activin-regulated homeo box gene. *Genes Dev.* **7**, 355-366.

Wallingford, J. B. and Harland, R. M. (2001). Xenopus Dishevelled signaling regulates both neural and mesodermal convergent extension: parallel forces elongating the body axis. *Development* **128**, 2581-2592.

Wallingford, J. B., Rowning, B. A., Vogeli, K. M., Rothbacher, U., Fraser, S. E. and Harland, R. M. (2000). Dishevelled controls cell polarity during Xenopus gastrulation. *Nature* **405**, 81-85.

Wallingford, J. B., Fraser, S. E. and Harland, R. M. (2002). Convergent extension: the molecular control of polarized cell movement during embryonic development. *Dev. Cell* **2**, 695-706.

Wilson, P. A., Oster, G. and Keller, R. (1989). Cell rearrangement and segmentation in Xenopus: direct observation of cultured explants. *Development* **105**, 155-166.

Zygar, C. A., Cook, T. L. and Grainger, R. M., Jr (1998). Gene activation during early stages of lens induction in Xenopus. *Development* **125**, 3509-3519.